Use of Symmetrical Peak Extraction in Drone Micro-Doppler Classification for Staring Radar

Cameron Bennett[&1], Mohammad Jahangir[†2], Francesco Fioranelli[%3], Bashar I Ahmad[*4], and Julien Le Kernec[&5]

[&]James Watt School of Engineering, University of Glasgow, Glasgow, UK

[†]School of Electronic, Electrical and Systems Engineering, University of Birmingham, Birmingham, UK

[%]Microwave Sensing Signals and Systems, Department of Microelectronics, TU Delft, Delft, The Netherlands

[*]Aveillant Limited, Cambridge, UK

[1]2193356B@student.gla.ac.uk, [2]m.jahangir@bham.ac.uk, [3]F.Fioranelli@tudelft.nl, [4]bashar.ahmad@aveillant.com, [5]julien.lekernec@glasgow.ac.uk

Abstract—**The commercialization of drones has granted the public with unprecedented access to unmanned aviation. As such, the detection, tracking, and classification of drones in radars have become an area in high demand to mitigate accidental or voluntary misuse of these platforms. This paper focuses on the classification of drone targets in a safety context where the concept of Explainable AI is of particular interest. Here, we propose a simple, yet effective, means to extract a salient symmetry feature from the micro-Doppler signatures of drone targets, arising from onboard rotary components. Most importantly, this approach maintains the explainable nature of the employed recognition algorithm as the symmetry feature is directly related to the kinematics of the drones as the targets of interest. A large dataset collected from multiple locations with over 280 minutes of rotary and fixed wing drone flights has been collected and used to demonstrate the generalization capability of this approach.**

Keywords—staring radar, drones, supervised learning, micro-Doppler, classification

I. INTRODUCTION

A. Background and Motivation

The increasing access to drone technology over the past decade has resulted in new technological adaptions that are beneficial in many sectors. However, this has led to an increased risk of this technology being exploited for malicious purposes. This has also caused an increased presence of drones in civilian airspace and interference with the day to day operation of airports. Events such as the closure of Gatwick in December of 2018 [1] and a hostile drone attack in Saudi Arabia in September 2019 [2] have publicized the need for counter-drone technology.

A key component of counter-drone technology is the non-cooperative detection of drones. Aveillant's Holographic staring radar technology has been proven to be particularly effective when detecting and tracking small drones [3]. However, the sensitivity of these radars enables them to track other small targets such as birds [4]. It is important to be able to discriminate between birds and drones to avoid too many false alarms. However, birds have similar flight characteristics, which make this discrimination a challenging task when exploiting only trajectory-based features [5].

Small airborne targets have been shown to exhibit distinguishing features in their frequency domain spectra that relate to their micro-Doppler signatures [6]. Drones that have rotating blades cause a modulation in addition to the main body Doppler, resulting in multiple micro-Doppler components. In contrast, birds that otherwise have a similar echo strength to drones tend to present with one or two components in their micro-Doppler responses due to the beating effect of their wings, especially at L-band as demonstrated in this paper. Birds can also fly in flocks, which results in Doppler signatures that may closely resemble a drone target. In this paper, a method is presented that distinguishes between these signatures by aligning micro-Doppler components with their associated target body. The symmetry of these components around the main body Doppler is utilized to counteract misleading signatures when multiple targets are present, e.g., birds of an RCS and flight profile similar to a drone. The introduced symmetry peak detection method is shown to provide unique feature separation between drones and other small airborne non-drone targets such as birds.

B. Related Work and Contributions

There have been several studies addressing the classification of drones in radar systems due to the increased demand for this technology [7]. A collection of these papers utilize a kinematic feature set that includes interpretable attributes such as velocity, acceleration, and curvature [5,8,9]. These studies have demonstrated how kinematic features can be employed as part of machine learning algorithms. However, these features alone do not offer significant enough distinction to be depended upon as part of explainable classification algorithms such as decision tree classifiers [9].

Another common approach has been to analyze the micro-Doppler components using deep learning. Various architectures such as Convolutional and Recurrent Neural Networks (CNN, RNN) have been shown to offer almost perfect classification results, but lack an interpretable nature [10,11]. As an alternative, there have been some handcrafted micro-Doppler features proposed that extract flight characteristics of drones. These include using the center of gravity to identify those targets with payloads from others, Principal Component Analysis (PCA) and eigenvector and eigenvalue decomposition of the micro-Doppler spectra [12,13,14]. This handcrafted feature extraction can be adopted alongside kinematic features to improve classification results in explainable classifiers.

This paper proposes a new feature that accounts for the shape and interaction of micro-Doppler components for different classes of targets while maintaining a very explainable nature. This feature has been designed to be

adopted as part of interpretable classifiers, such as those proposed in [8] and offers a unique separation between drones and other targets. In order to demonstrate the robust nature of this feature, a substantial dataset has been collected of diverse experimental signatures containing data from fixed wing and rotary wing drones from three different locations and for flights up to 2.6 km radar range. The interpretable classification algorithms achieve comparable accuracy to more complex black box approaches such as RNNs or CNNs.

The remainder of this paper is organized as follows. Section II gives an overview of the Aveillant Holographic staring radar that was used to collect data. Section III highlights the intuition behind the symmetry feature through analysis of micro-Doppler signatures. An outline of feature extraction is given in Section IV followed by classification results in Section V with conclusion drawn in Section VI.

II. Staring Radar System Overview

Data collected with the Aveillant Gamekeeper 16U drone detection radar [3,4] is used in signature characterization, feature extraction, and target classification for non-cooperative surveillance of small targets. The Gamekeeper 16U is a staring system specifically designed for high-performance detection of drones. The transmitter uses a broad beam antenna to illuminate the entire search volume. A 16x4 array of receiver elements are arranged in a 2-D grid pattern that allows the radar to continuously stare in all directions so that it is able to process echoes by forming simultaneous beams that cover the entire search volume. The staring aspect of this radar allows it to have long, customizable dwell times, which results in fine Doppler resolution. This provides enhanced detection and discrimination of slow-moving drones against stationary clutter. Previous work has reported the capabilities of such a radar against typical drone targets [15].

The Gamekeeper 16U radar (Figure 1), has a vertical stack of 8 transmit antennas to narrow the illumination beam in elevation, thereby providing more gain at low altitudes. This provide better sensitivity against low altitude, low observable targets. TABLE I. lists the operating parameters for the Gamekeeper 16U sensor.

Figure 1: Aveillant Gamekeeper 16U multi-beam staring radar.

Parameter	Value
Frequency	L band
Bandwidth	~2 MHz
Transmit power	~1 kW
Receiver channels	4 x 16
Azimuth coverage	90°
Elevation coverage	30°
Pulse Repetition Frequency (PRF)	~7.5 kHz
Update rate	~0.25 s
Polarisation	Vertical
Drone detection range	5 km

The radar transmits a pulsed waveform, which is backscattered to the receiver array and is digitized at each receiver element. For each range gate, the samples from all the receiver channels are processed to form multiple receive beams. Pulses from a time frame of 279 milliseconds are coherently processed in a 2048-point FFT to obtain Doppler samples, thus providing a 4-D data matrix in range, azimuth, elevation, and Doppler for each frame. Here each frame is equivalent to one Coherent Processing Interval (CPI), which is 279 milliseconds. CFAR thresholding is applied to each 4-D frame, and the detections are localized in position. After some pre-tracker filtering, detections are passed to a tracker that assigns track IDs. Feature values are generated for each track for each frame update. The track features are derived both from the kinematic features and also contain features relating to the Doppler spectrum. Earlier work has only considered the number of Doppler harmonics that can be attributed to a tracked target [6,8,15]. The Doppler feature extraction is performed using a dedicated module that detects the number of micro-Doppler components corresponding to a given track. These tracker features are used by a classifier to assign the class label, and the classification label is updated each frame for all tracks. The radar creates tracks with their track ID, positional information, and classification labels at a per frame update rate.

However, a simple representation of the micro-Doppler components for example [11] does not capture the more detailed information regarding the pattern of the micro-Doppler spectral components characteristic of multi-rotor drones (See Section III). In this paper, we present a peak extraction method able to quantify specific symmetries in the micro-Doppler signatures of drones that is evidently absent in birds and other non-drone confuser targets. This method is shown to provide more robust Doppler features that can improve discrimination of drone tracks from birds and other confuser tracks.

III. MICRO-Doppler signatures of drones and non-drones

In radars using short dwell, the spectrograms of drone echoes can create flashes caused by the rotating motion of the blades. Approaching and receding ends of the blade and other effects are modulated into continuous harmonics that are commonly referred to as Helicopter Rotor Modulation (HRM) lines. The Doppler harmonics are quite typical where

the dwell time is relatively long [17]. An example spectrogram of a rotary DJI Inspire I drone is shown Figure 2. Each Doppler profile is a time frame corresponding to 279 milliseconds. The vertical axis is time plotted as frame number.
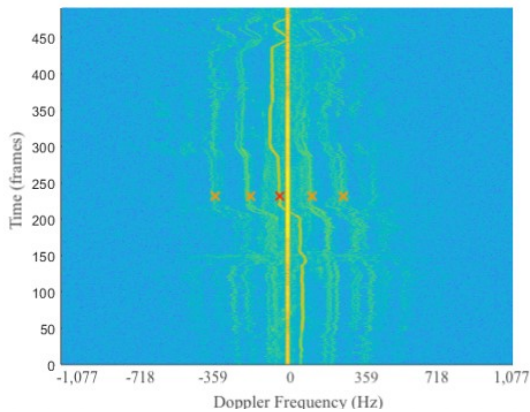

Figure 2: Spectrogram of DJI Inspire 1 rotary wing drone.

The red cross in Figure 2 indicates the Doppler component associated with the main body of the drone while the orange crosses indicate the micro-Doppler components caused by the rotors. There are two distinct trends in this spectrogram. The first is the sideband-carrier effect of the body and its rotor components. This is caused by the relative speed of the target's rotors relative to its main body mean speed, therefore, displaying modulation around the mean Doppler of the drone. The second is a consistent symmetrical scattering of the rotor harmonics around the main body's Doppler shift. The approaching and receding blades create a positive and negative Doppler shift that are equal, but opposite to one another.

Contrast the drone spectrum with that from a bird, as shown in Figure 3. This target was tracked for over 600 frames, and the red cross indicates the Doppler component associated with the main body. There are no distinct Doppler sidebands visible. Although there are some additional Doppler echoes present, these are random and are most likely the result of the Doppler return from other nearby birds.
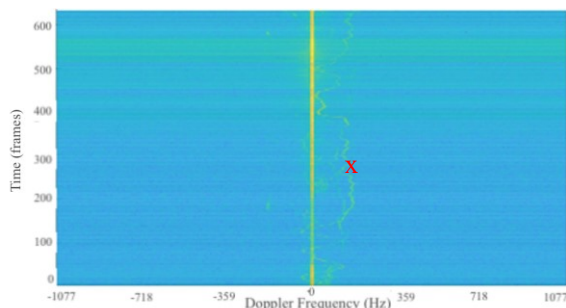

Figure 3: Spectrogram of a bird.

A common approach for incorporating micro-Doppler components in an explainable drone classifier is to count the number of these components [6,8,15]. Drones typically exhibit four or more, whereas birds usually have only two components at most. A potential problem with this approach is that birds often fly in flocks, which can result in a wide variety of Doppler activity. It is therefore important to be able

to associate micro-Doppler motions with the correct target body and distinguish whether these are being caused by a single target or multiple targets. The micro-Doppler components caused by drone blades have been observed in symmetrical pairs around the main body and are a useful distinguishing feature [21]. This means that misconceptions caused by multiple targets flying close together can be mitigated by identifying whether each component has an associated symmetric partner.

IV. PEAK EXTRACTION METHOD

To capture the degree of symmetry in the Doppler components, a peak extraction approach was developed to highlight large rotor returns. Peaks are identified in a single timestep of the target spectrogram using minimum prominence and width. This is implemented using SciPy's peak finding tool [16] which identifies local maxima by a simple comparison with neighbouring values. The prominence of a peak indicates how much the peak stands out and is defined as its height over adjacent minima. This is depicted graphically in Figure 4 by the vertical orange lines. The algorithm identifies prominence by comparing the tallest adjacent minima to the selected peak. The width of a peak is measured at half the prominence of each peak and is indicated by the horizontal orange lines. These values were optimized to ignore unwanted peaks from background sources. Each peak that is recorded is checked to identify whether it has the largest magnitude within its vicinity. If not, then it is discarded. This avoids components with large widths being counted as multiple peaks.
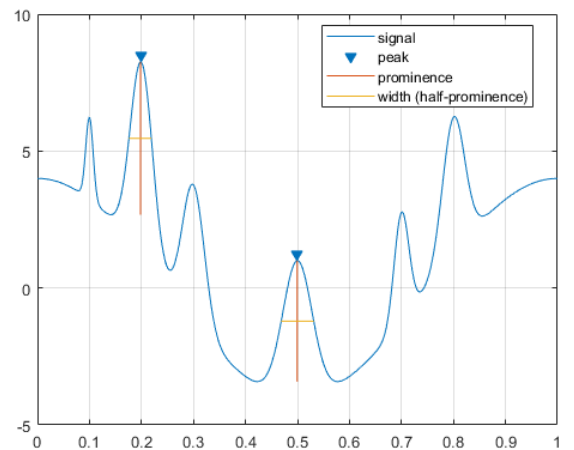

Figure 4: Diagram illustrating peak prominence and width. Orange vertical and horizontal lines indicate prominence and width[20].

In order to extract the symmetry of these components, the main body Doppler component must be identified such that it can be used as a central reference. Its Doppler shift is calculated using the range rate provided by the tracker and is established as the central mirror point. Dominant peaks at zero Hz caused by background clutter are ignored unless the main body's Doppler shift crosses this point. Symmetric peaks are then identified in an iterative fashion by sequentially checking each peak for a partner that mirrors the target's body. A window is used when checking these peaks so that small discrepancies in the position of these components are still recorded as a symmetric pair. Figure *5*

shows an example of the peaks extracted using this approach when tested on a single time frame from the drone spectrogram in Figure 2.
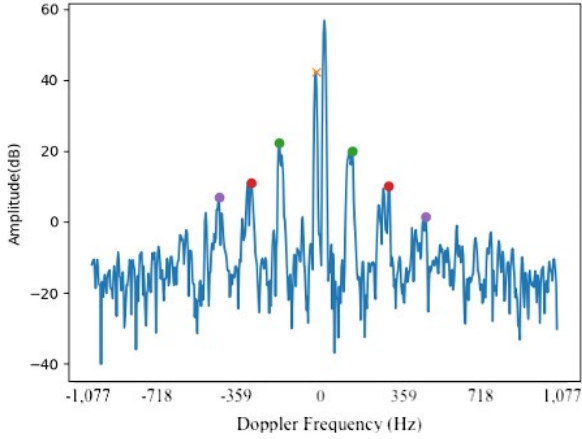

Figure 5: Example of symmetry feature extraction applied to a single frame from the drone spectrum. The orange cross shows extracted main body and colored dots show extracted symmetric micro-Doppler pairs.

The colored dots in Figure 5 indicate the peaks that have been chosen as symmetric pairs, and the orange cross shows the main body component. Each pair of colored dots is counted as a single symmetric pair, and the total number of symmetrical components for each timestep are outputted to be used as a feature. This process is summarized in the pseudo-code written in Figure 6.

```
Algorithm 1: Pseudocode for symmetry feature extraction.
1  function symmetryFeatureExtract (s);
   Input  : Frequency spectrogram s of target trajectory.
   Output: Symmetry count at each time frame symmetryFeature.
2  for timeFrame in s do
3  |   peaks = findPeaks(s,prominence, width, adjacentDistance);
4  |   dopplerBin = getDopplerBin(rangeRate);
5  |   while peaks[i] <dopplerBin do
6  |   |   if mirrored(peaks[i], dopplerBin) then
7  |   |   |   symmetryCount++
8  |   |   end
9  |   |   i++
10 |   end
11 |   symmetryFeature[timeFrame] = symmetryCount
12 end
```

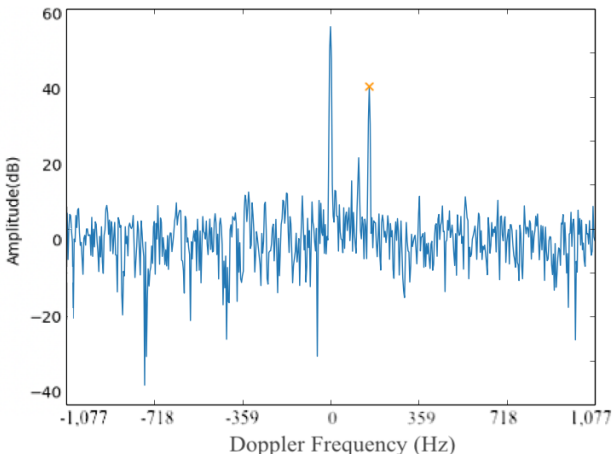*Figure 6: Pseudocode for symmetry feature extraction.*

Figure 7: Example of symmetry feature extraction applied to a single frame from a bird spectrum. The orange cross marks the peak corresponding to the Doppler of the main body.

As a comparison, Figure 7 shows the result of the peak extraction applied to one frame of the bird spectrum from Figure 3. The algorithm detected the target main body return as marked by the orange cross. However, in this case, whilst there were some minor peaks in the Doppler spectrum, there were no reported symmetrical peaks, and hence the algorithm reports zero symmetrical peaks.

V. RESULTS ON EXPERIMENTAL DATA

A. Evaluation Dataset

In order to evaluate this approach, a large dataset containing over 280 minutes of drone flights was collected. The flights in these recordings span many days of trials in two different locations out to a maximum range of 2.6 km. Flights were conducted using a DJI Inspires 1 and 2 as part of the SESAR CLASS [9] and SESAR SAFIR [8] consortiums trials program and as such, were recorded in a live setting without any optimization or conditioning of the surrounding environment. The 55 flights that are included in this dataset make up for 34% of the data, with other background targets such as birds filling the rest. The details of this dataset are shown in TABLE II.

TABLE II.   DATASET CONTENT DESCRIPTION

Reference Dataset Parameters	
Class Balance	34% Drone
Train : Test	80 : 20
Drone Flights	55
Total Flight Time (mins)	282
Datapoints(PRIs)	178135
Size (GB)	7.4
Locations	Deenethorpe, Antwerp
Range Span (Km)	0.76 - 2.58

B. Results

The number of symmetrical pairs is recorded for each time frame. A single symmetrical pair refers to micro-Doppler components that mirror each other. Figure 8 shows the histogram of the number of symmetrical components between drone and non-drone targets for all considered flights. Non-drone targets mostly display zero symmetrical pairs, but a significant portion has a single pair. This is likely due to the beating of bird wings, causing a mirrored pair. There is a very clear separation of drone vs. non-drone targets using this feature at two components. Owing to the good separation between the target classes means that a simple hard threshold put on this feature at two components is able to achieve a True Positive Rate (TPR) of 91.4% for drones and True Negative Rate (TNR) of 96.4% for non-drones. This is excellent separation considering that this is based upon a single feature. The histogram for the number of micro-Doppler components, i.e., without counting pairs of symmetric peaks, is shown in Figure 9 for comparison. This shows that the distinction between the two classes of interest is far clearer when using the symmetry feature.
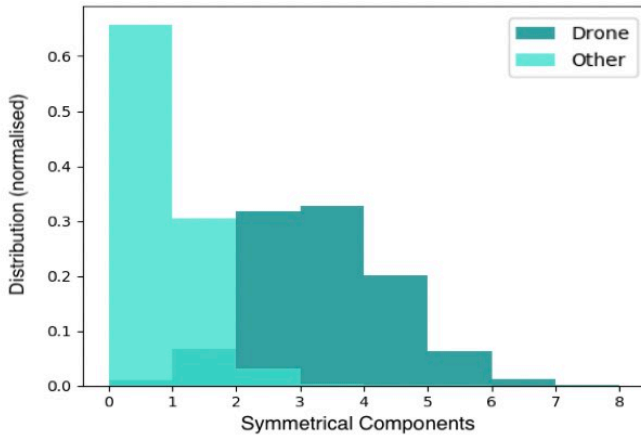
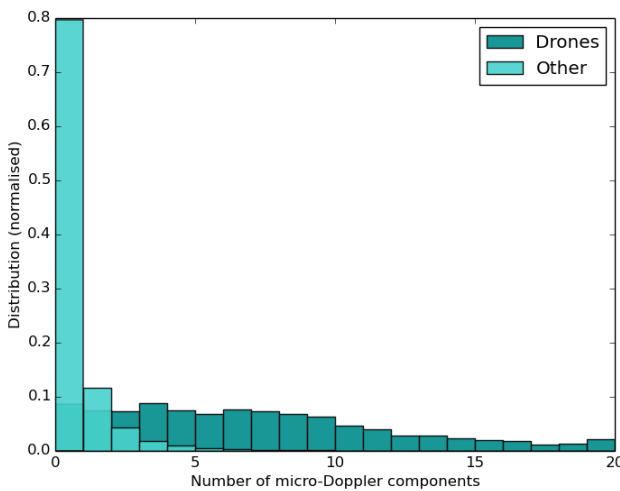*Figure 8: Symmetrical components (normalized) histogram for drone and other targets.*

Figure 9: Number of micro-Doppler components (normalized) histogram for drones and other targets.

A decision tree was trained with this feature along with four other interpretable features: height, velocity, the total number of micro-Doppler components, and the Radar Cross Section (RCS). No limit was used on the number of nodes or the depth of the tree, 80% of the dataset was used for training with the rest being used for testing. The importance of each feature in this decision tree was calculated using SciKit-Learn's Importance tool [18]. This tool determines how much a given feature contributes to the final classification and outputs this as a single importance value. This calculation is based on using Gini impurity [19], which evaluates each node based on the frequency of their evaluation on a given feature. By analyzing how heavily the decision tree weights its classification on each feature, a fair comparison can be made between each of the explainable features. Figure 10 shows the importance values for each of the features used to train the decision tree. No limit was set on the number of layers in this tree, and so the final tree contained 15 layers.

The decision tree weighted a very heavy dependence on the proposed symmetry feature. One particularly interesting aspect of these important values is that the tree weighted the symmetry with more than six times the importance than it did for the number of micro-Doppler components. This indicates that the relative shape and interaction of these components is substantially more important than just the number of micro-

Doppler components. The confusion matrix for this decision tree that was trained with the proposed symmetry feature is shown in TABLE III. The inclusion of the proposed feature in the decision tree increased the TPR by 5% and reduced the FPR from 0.38% to 0.19% when compared to the result obtained using a decision tree trained without the symmetry feature (TABLE IV).
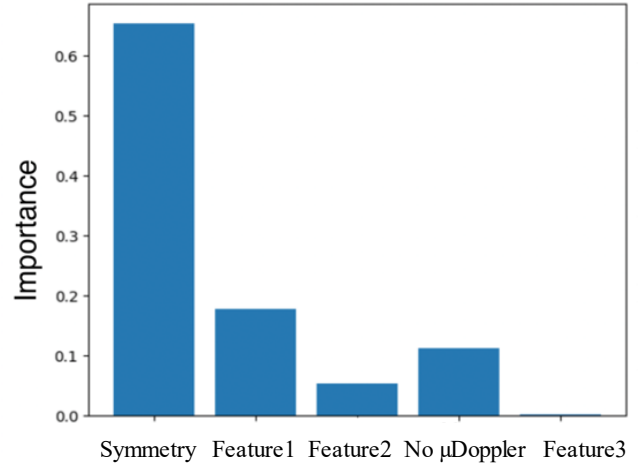

Figure 10: Importance values assigned to each feature in the decision tree.

TABLE III.   CONFUSION MATRIX FOR DECISION TREE CLASSIFIER WITH SYMMETRY FEATURE

		Predicted Class	
		Drone	Other
True Class	Drone	95.71	4.29
	Other	0.19	99.81

TABLE IV.   CONFUSION MATRIX FOR DECISION TREE CLASSIFIER WITHOUT SYMMETRY FEATURE

		Predicted Class	
		Drone	Other
True Class	Drone	90.40	9.60
	Other	0.34	99.66

Having established an encouraging classification capability based on signatures of rotary wing drones, data from a fixed-wing model aircraft was recorded to test whether this feature can generalize well to such platforms. Figure 11 shows the histogram of symmetrical components with the fixed-wing drone included. The distinction between drone and non-drone targets is still very clear at two components. In general, the fixed-wing exhibits considerably more symmetrical components than the rotary drones. The increase in Doppler activity can be possibly attributed to the higher rotation rate of the fixed-wing drones compared to rotary wing drones. A TPR of 92.81% was observed with a hard

decision threshold at two components showing that this feature can generalize between rotary and fixed-wing drones.
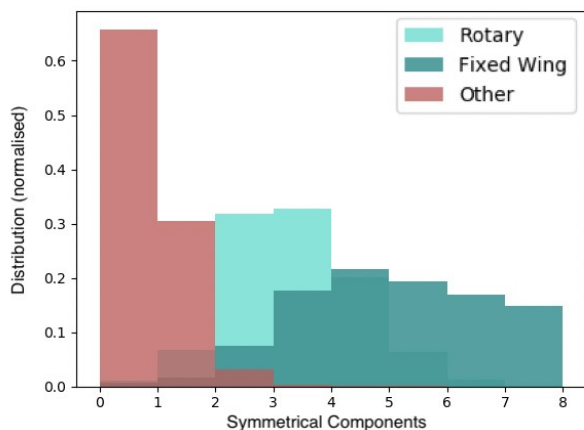

Figure 11: Histogram of symmetrical components that includes fixed-wing drone.

VI. CONCLUSION

This paper has proposed a symmetry feature that exploits the mirrored effect of approaching and receding drone propellor blades. The intuition behind this feature is to offer a simple way to encapsulate the shape and interaction of micro-Doppler components in order to determine whether targets are man-made or not. In contrast to deep learning approaches, the explainable nature of this feature means that it can be adopted as part of systems in industries that must conform with Explainable AI. It is common for flocks of birds to cause large amounts of micro-Doppler activity, which can make only counting the number of these components an unreliable feature. It has been shown that the proposed feature can distinguish between these targets by extracting the relationship between micro-Doppler components and the target's main body.

The feature has been shown to offer a distinct separation between drones and other targets. Over 92% of the drone in the data set were observed to have two or more symmetric pairs. This level of separation in a single feature is uncommon and has been shown to generalize across a large dataset with both rotary and fixed-wing models. The inclusion of this feature in a decision tree was shown to improve the classification performance when using the number of micro-Doppler components by 5% TPR. The histograms of this feature also indicate that the symmetry would also enhance the performance of Bayesian classifiers.

Despite the promising separation provided by this feature, there are further developments that will be explored in future work. The optimization of this feature for low Signal-to-Noise Ratio (SNR) conditions is a primary objective going forward, and a dynamic version of this feature could be developed to adapt the algorithm based on characteristics that impact the SNR, such as the target range. In order to thoroughly test this, more data at a longer range could be used to demonstrate whether this feature can robustly classify targets with low Doppler returns.

ACKNOWLEDGMENT

REFERENCES

[1] The Guardian, "Military called in to help Gatwick drone crisis", Dec. 2018, URL: https://www.theguardian.com/uknews/2018/dec/19/gatwick-flights-halted-after-drone-sighting, (Accessed 15 Mar. 2020).

[2] The British Broadcasting Corporation, "Shooting drones out of the sky with Phasers", Oct. 2019, URL: https://www. bbc.co.uk/news/business-49984415, (Accessed 20 Nov. 2019).

[3] M. Jahangir and C. J. Baker, "Persistence Surveillance of Difficult to Detect micro-drones with L-band Holographic Radar", *CIE 2016 Int. Radar Conf.*, Guangzhou, China, Oct. 2016.

[4] M. Jahangir and C. J. Baker, "Characterisation of low observable targets with a multi-beam staring radar", *IET Radar 2017*, Belfast, UK, Oct. 2017.

[5] S. Bækkegaard, J. Blixenkrone-Møller, J. J. Larsen and L. Jochumsen, "Target Classification Using Kinematic Data and a Recurrent Neural Network", *Intern. Radar Symposium IRS 2018*, Bonn, Germany, Jun. 2018.

[6] M. Jahangir and C. J. Baker, "Extended dwell Doppler characteristics of birds and micro-UAS at L-Band", *Intern. Radar Symp. IRS 2017*, Prague, Czech Republic, Jun. 2017.

[7] J. S. Patel, F. Fioranelli and D. Anderson, "Review of radar classification and RCS characterisation techniques for small UAVs or drones," in *IET Radar, Sonar & Navigation*, vol. 12, no. 9, pp. 911-919, 9 2018.

[8] M. Jahangir, B.I. Ahmad and C.J. Baker, " Robust Drone Classification Using Two-Stage Decision Trees and Results from SESAR SAFIR Trials", *IEEE International Radar Conference*, Washington, US, Apr. 2020.

[9] M. Jahangir and C. J. Baker, "CLASS U-space drone test flight results for non-cooperative surveillance using an L-band 3-D staring radar", *Intern. Radar Symposium IRS 2019*, Ulm, Germany, Jun. 2019.

[10] H. Dale, C.J. Baker, M. Antoniou and M. Jahangir, "An Initial Investigation into Using Convolutional Neural Networks for Classification of Drones", *IEEE International Radar Conference*, Washington, US, Apr. 2020.

[11] P. Molchanov, R. I. Harmanny, J. J. de Wit, K. Egiazarian and J. Astola, "Classification of small UAVs and birds by micro-Doppler signatures", *Intern. Journal of Microwave and Wireless Technologies*, vol. 6, issue 3-4, pp. 435–444, 2014.

[12] F.Fioranelli et al. "Classification of loaded/unloaded micro-drones using multistatic radar", *Electronics Letters* 51.22, Oct. 2015.

[13] P. Zhang et al. "Classification of drones based on micro-Doppler signatures with dual-band radar sensors", *Progress in Electromagnetics Research Sym- posium 2017*, Nov. 2017.

[14] P. Molchanov et al. "Classification of small UAVs and birds by micro-Doppler signatures", *International Journal of Microwave and Wireless Technologies* 6.3-4 Oct. 2013.

[15] M. Jahangir and C. J. Baker, "L-band staring radar performance against micro-drones", *Intern. Radar Symposium IRS 2018*, Bonn, Germany, Jun. 2018.

[16] SciPy, "scipy.signal.find_peaks SciPy.org Documentation", URL: https://docs.scipy.org/doc/scipy/reference/generated/scipy.signal.find_peaks.html (Accessed Dec. 2019).

[17] Samiur Rahman, Duncan A. Robertson, "Millimeter-wave micro-Doppler measurements of small UAVs," Proc. SPIE 10188, *Radar Sensor Technology XXI*, 101880T, May. 2017.

[18] SciKit Learn, "Feature Importance: sklearn.tree DecisionTreeClassifier", URL:https://scikit-learn.org/stable/modules/generated/sklearn.tree.DecisionTreeClassifier.html#sklearn.tree.DecisionTreeClassifier.feature_importances_ (Accessed Dec. 2019).

[19] C. Lee, Medium, Oct. 2017, URL:https://medium.com/the-artificial-impostor/feature-importance-measures-for-tree-models-part-i-47f187c1a2c3 (Accessed Dec. 2019).

[20] MathWorks, Peak Prominence, URL: https://uk.mathworks.com/help/signal/ref/findpeaks.html (Accessed Dec. 2019).

[21] Stephen Harman, "Analysis of the radar return of micro-UAVs in flight", *2017 IEEE Radar Conference*, Seattle, USA, May 2017.